

Differential Recognition of Deacetylated PNAG Oligosaccharides by a Biofilm Degrading Glycosidase

Shaochi Wang, Alexandra P. Breslawec, Elaine Alvarez, Michal Tyrlik, Crystal Li, and Myles B Poulin

ACS Chem. Biol., **Just Accepted Manuscript** • DOI: 10.1021/acscchembio.9b00467 • Publication Date (Web): 20 Aug 2019

Downloaded from pubs.acs.org on August 26, 2019

Just Accepted

“Just Accepted” manuscripts have been peer-reviewed and accepted for publication. They are posted online prior to technical editing, formatting for publication and author proofing. The American Chemical Society provides “Just Accepted” as a service to the research community to expedite the dissemination of scientific material as soon as possible after acceptance. “Just Accepted” manuscripts appear in full in PDF format accompanied by an HTML abstract. “Just Accepted” manuscripts have been fully peer reviewed, but should not be considered the official version of record. They are citable by the Digital Object Identifier (DOI®). “Just Accepted” is an optional service offered to authors. Therefore, the “Just Accepted” Web site may not include all articles that will be published in the journal. After a manuscript is technically edited and formatted, it will be removed from the “Just Accepted” Web site and published as an ASAP article. Note that technical editing may introduce minor changes to the manuscript text and/or graphics which could affect content, and all legal disclaimers and ethical guidelines that apply to the journal pertain. ACS cannot be held responsible for errors or consequences arising from the use of information contained in these “Just Accepted” manuscripts.

Differential Recognition of Deacetylated PNAG Oligosaccharides by a Biofilm Degrading Glycosidase

Shaochi Wang, Alexandra P. Breslawec, Elaine Alvarez, Michal Tyrlik, Crystal Li and Myles B. Poulin*

Department of Chemistry and Biochemistry, University of Maryland, College Park, Maryland 20742, United States

ABSTRACT: Exopolysaccharides consisting of partially de-*N*-acetylated poly- β -D-(1 \rightarrow 6)-*N*-acetyl-glucosamine (dPNAG) are key structural components of the biofilm extracellular polymeric substance of both gram-positive and gram-negative human pathogens. De-*N*-acetylation is required for the proper assembly and function of dPNAG in biofilm development suggesting that different patterns of deacetylation may be preferentially recognized by proteins that interact with dPNAG, such as Dispersin B (DspB). The enzymatic degradation of dPNAG by the *Aggregatibacter actinomycetemcomitans* native β -hexosaminidase enzyme DspB plays a role in biofilm dispersal. To test the role of substrate de-*N*-acetylation on substrate recognition by DspB, we applied an efficient pre-activation based one-pot glycosylation approach to prepare a panel of dPNAG trisaccharide analogs with defined acetylation patterns. These analogs served as effective DspB substrates and the rate of hydrolysis was dependent on the specific substrate de-*N*-acetylation pattern, with glucosamine (GlcN) located +2 from the site of cleavage being preferentially hydrolyzed. The product distributions support a primarily exoglycosidase cleavage activity following a substrate assisted cleavage mechanism, with the exception of substrates containing a non-reducing GlcN that were cleaved *endo* leading to the exclusive formation of a non-reducing disaccharide product. These observations provide critical insight into the substrate specificity of dPNAG specific glycosidase that can help guide their design as biocatalysts.

INTRODUCTION

Biofilms consisting of surface associated bacteria imbedded in an extracellular polymeric substance (EPS), are responsible for approximately 65% of all human bacterial infections.¹ The EPS is composed of exopolysaccharides, proteins and extracellular DNA, that facilitate cell-cell attachment and provide a protective barrier against antibiotics and the host immune system.²⁻⁶ Many medically important biofilm forming bacterial strains, including *Staphylococcus epidermidis*,² *Staphylococcus aureus*,³ *Escherichia coli*,⁴ *Acinetobacter baumannii*,⁵ *Actinobacillus pleuropneumoniae*,⁶ *Klebsiella pneumoniae*,⁷ and *Yersinia pestis*,⁸ produce a similar partially de-*N*-acetylated poly- β -D-(1-6)-*N*-acetyl-glucosamine (dPNAG) as the key EPS exopolysaccharide. In these organisms dPNAG functions as a major virulence factor, and contributes to pathogenicity in animal infection models.⁹ Partial deacetylation of PNAG by specific carbohydrate esterase enzymes plays a role in the proper export and function of dPNAG in biofilms of gram-negative bacteria and is required for proper cell association in gram-positive bacteria,⁹⁻¹² yet the exact function of deacetylation is poorly understood. Specifically, it is not clear if deacetylation impacts binding and recognition of dPNAG by other proteins.

Enzymes that breakdown the biofilm EPS, including glycosidase, DNase and protease enzymes have emerged as promising tools to disrupt existing biofilms.¹³⁻¹⁶ DispersinB (DspB), specifically, is a native *Aggregatibacter actinomycetemcomitans* β -hexosaminidase enzyme specific for the hydrolysis of dPNAG polysaccharides,¹⁷ and has been used to catalyze biofilm dispersal *in vitro* for a number of

biofilm forming bacteria.^{18,19} DspB is a member of the CAZy GH20 family of glycosyl hydrolase enzymes,^{20,21} and is one of only two enzyme specific for dPNAG hydrolysis identified.²² The other, PgaB contains a C-terminal CAZy GH153 family of glycosyl hydrolase that catalyzes the endoglycosidic cleavage of dPNAG containing de-*N*-acetylated GlcN in the -3 binding site using a yet unidentified cleavage mechanism.²² Compared to PgaB, the specific interactions required for dPNAG binding and recognition by DspB remain poorly understood. dPNAG hydrolysis by DspB likely follows a substrate assisted cleavage mechanism in which the substrate 2-acetamido group facilitates glycoside hydrolysis through formation of a characteristic oxazolinium ion intermediate (Figure 1A),²³ which is characteristic of GH20, 18, 25, 56, 84, and 85 family enzymes.²⁴ All studies of DspB activity have used either isolated PNAG polysaccharides containing a heterogeneous distribution of acetylated and deacetylated GlcNAc,^{17,19} or synthetic PNAG oligosaccharides composed entirely of acetylated GlcNAc.^{25,26} From these studies it is not clear how DspB cleaves the 3-20% deacetylated GlcN present in native dPNAG polysaccharides,²⁷ which lack a 2-acetamido group required for substrate assisted cleavage. Studying the role of deacetylation for PNAG hydrolysis by DspB requires PNAG oligosaccharides with chemically defined acetylation patterns (Figure 1B).

Unlike direct isolation from bacterial biofilms, chemical synthesis provides access to deacetylated PNAG in relatively large scale.³²⁻³⁵ Previous approaches to synthesize fully acetylated PNAG oligosaccharides have employed convergent approaches,^{25,28-32} acid reversion chemistry,³³ one-

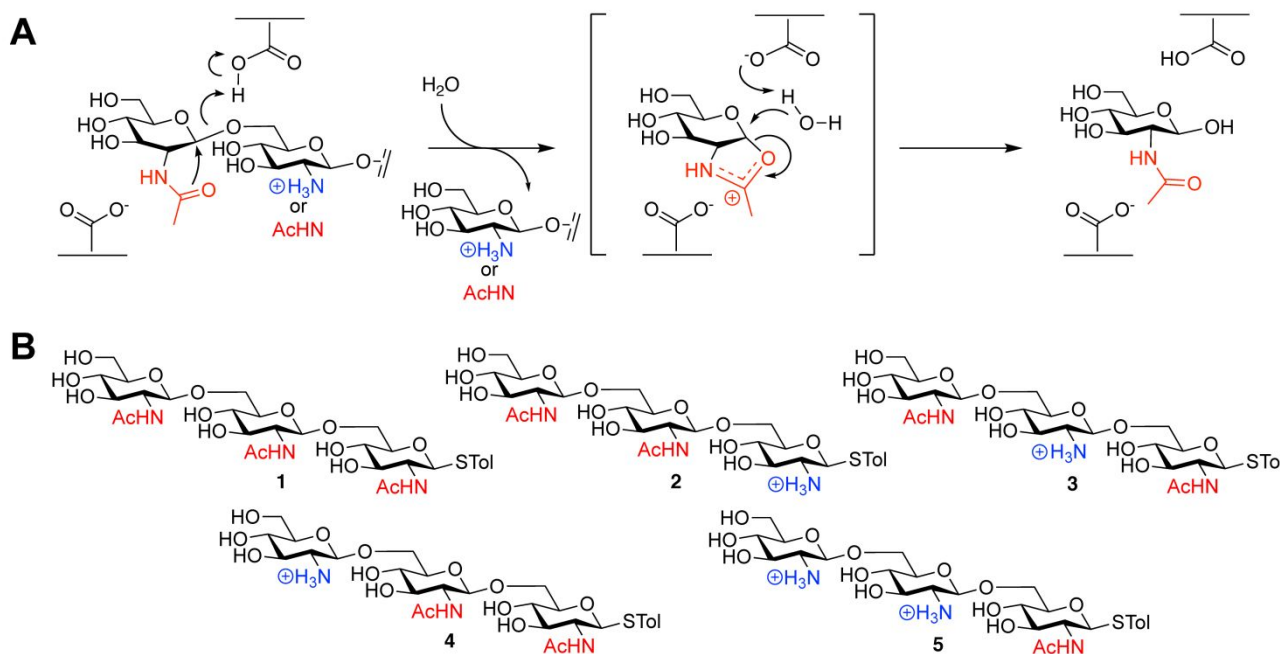


Figure 1. Mechanism of dPNAG hydrolysis catalyzed by DspB. (A) dPNAG hydrolysis is proposed to involve substrate assisted cleavage characterized by formation of an oxazolinium ion intermediate. (B) Structure of dPNAG trisaccharide analogs with defined acetylation patterns synthesized to probe DspB specificity.

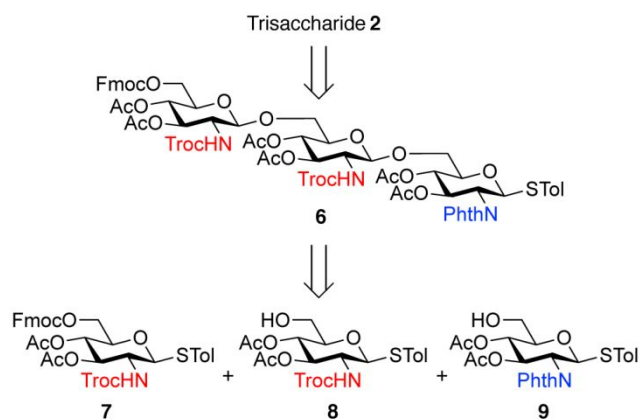


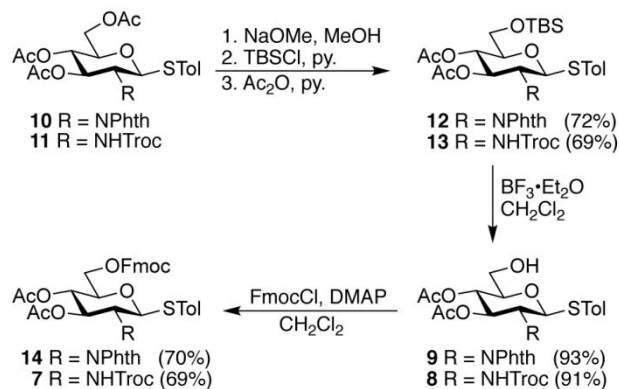
Figure 2. Retrosynthetic analysis of trisaccharide 2. The selectively protected trisaccharide 5 can be prepared using a combination of glycosyl donor 7 with glycosyl acceptors 8 and 9 with orthogonal nitrogen protection. The remaining trisaccharide analogs are prepared in an analogous manner using the same building blocks.

pot glycosylation reactions,³⁴ automated synthesis,³⁵⁻³⁷ and non-specific polymerization reactions.³⁸ However, these methods produced either uniformly acetylated PNAG derivatives or dPNAG with random de-*N*-acetylation, with only one example of dPNAG synthesis with defined de-*N*-acetylation reported,³⁹ and there the GlcN content was far higher than in dPNAG samples isolated from bacterial species. Thus, there is a need for efficient methods to prepare deacetylated PNAG oligosaccharides as functional probes for dPNAG-protein interactions.

Compared to other methods, the pre-activation based glycosylation reactions developed by Huang *et al.* provides

a general one-pot approach to oligosaccharide synthesis that is independent of glycosyl donor reactivities.⁴⁰ This

Scheme 1. Synthesis of Monosaccharide Building Blocks



glycosylation approach has been successfully employed to prepare complex oligo- and polysaccharides.^{41,42} Here we present the synthesis of PNAG trisaccharides (1-5) with defined acetylation patterns using a pre-activation based one-pot strategy. The product trisaccharides were tested as substrates for DspB hydrolysis by evaluating both the rate of hydrolysis and product distribution. The results support a mechanism in which the dPNAG substrate acetylation patterns influence their recognition and mechanism of hydrolysis by DspB.

RESULTS AND DISCUSSION

Retrosynthesis. The retrosynthesis of trisaccharide 2, illustrated in Figure 2, demonstrates our general approach to assemble PNAG analogs with defined acetylation

patterns. The desired trisaccharide analogs **1–5** are accessible using the same glucosamine derived glycosyl donors, and glycosyl acceptors **8** and **9** with the primary amine orthogonally protected as *N*-phthalamide or *N*-Troc. Both serve as participating protecting groups allowing for high β -selectivity during glycosylation reactions. The *N*-Troc of **6** can be selectively removed under reductive conditions and acetylated *in situ* in the presence of *N*-Phth protection resulting in trisaccharides with defined acetylation patterns. An orthogonal protecting group (i.e. fluorenylmethyloxycarbonyl (Fmoc)), was incorporated onto the 6-OH of donor **7** to provide the flexibility to further apply the trisaccharide products (i.e. **6**) as glycosyl donors or alternatively deprotect the Fmoc to obtain glycosyl acceptors for preparing longer PNAG derivatives.

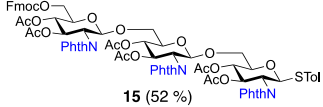
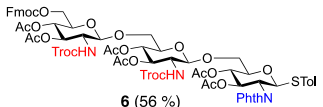
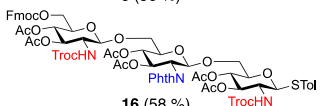
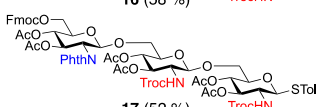
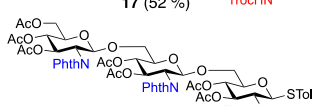
Building block synthesis. Based on this retrosynthetic approach, two monosaccharide glycosyl acceptors **8** and **9** containing a free 6-OH group and two fully protected glycosyl donors **7** and **14** (Scheme 1) were synthesized. The *O*-acetyl groups of thioglycoside **10**, prepared as previously described,⁴³ were first removed followed by a selective protection of the primary hydroxyl as the tert-butyltrimethylsilyl ether and *in situ* *O*-acetylation to afford the thioglycoside **12** in 72% yield over three steps. Silyl ether hydrolysis for **12** under acidic conditions yielded glycosyl acceptor **9**⁴⁴ in a 93% yield. Donor **12** was initially explored as a glycosyl donor, however, its activation with *p*-TolSCL and AgOTf resulted in its quantitative conversion to the 1,6-anhydrosugar (data not shown). Instead, Fmoc protection of the primary alcohol of **9** afforded glycosyl donor **14** in 70% yield. Starting from thioglycoside **11**,⁴³ the *N*-Troc protected thioglycoside donor **8**⁴⁵ and glycosyl acceptor **7** were synthesized in an analogous manner in 63% and 43% overall yields, respectively.

Iterative one-pot glycosylation. The one-pot assembly of fully protected trisaccharide analogs was performed as outlined in Table 1, using a pre-activation based one-pot sequential glycosylation approach.⁴⁰ Briefly, stoichiometric pre-activation of donors **7**, **10** or **14** with freshly distilled *p*-TolSCL in the presence of AgOTf (3 eq) at -78°C was followed by addition of the first acceptor (**8** or **9**) and the temperature raised to 0°C over 20 min. After complete consumption of the acceptor, as judged by TLC analysis, the reaction mixture was returned to -78°C followed by sequential addition of AgOTf, *p*-TolSCL, and a second acceptor (**8** or **9**). Warming to 0°C over 20 min gave protected trisaccharides **6** and **15–18** in isolated yields of 49–58% after flash column chromatography. The remaining material largely consisted of hydrolyzed donors. It is noteworthy that the reaction efficiency was not significantly affected by differences in the anomeric reactivity for each glycosyl donor. Thus, all orthogonally protected trisaccharide analogs could be obtained via the same approach by simply varying the order of substrate addition with little impact on product yield.

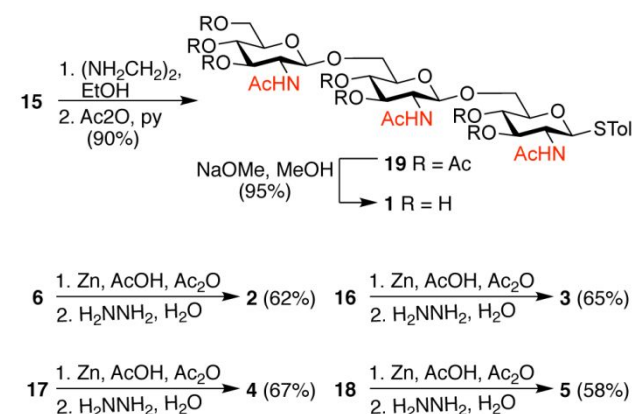
Selective deprotection. Per-*N*-acetylated trisaccharide **1** was obtained by treating **15** with ethylenediamine in refluxing ethanol followed by per-acetylation resulted in the isolation of trisaccharide **19** in 90% yield (scheme 2). This was followed by Zemplén deacetylation to give **1** in 95% yield. For access to analogs **2–5**, we developed a

selective deprotection and *N*-acetylation sequence outlined in scheme 2. Oxidative cleavage of the *N*-Troc protecting groups using pre-activated zinc dust under acidic conditions and *in situ* *N*-acetylation by acetic anhydride followed by global deprotection using aqueous hydrazine gave the product trisaccharides **2–5** in 58–62% yield over 2 steps, following recrystallization. Each trisaccharide analog was obtained in >95% purity as estimated from NMR and HPLC analysis and showed no evidence of *N*-Ac group migration during the reaction and purification. This approach provided rapid access to a panel of five PNAG trisaccharide analogs with defined acetylation patterns using the same glycosyl donors and acceptor molecules in sufficient quantities to facilitate their evaluation as substrates for DspB.

Table 1. Pre-activation based iterative one-pot glycosylation.

| donor | acceptor | | Product (% yield) |
|-------------|--|---|---|
| | 1 | 2 | |
| 7, 10 or 14 | $\xrightarrow[5\text{ min } -78^\circ\text{C}]{p\text{-TolSCL, AgOTf}}$ $\xrightarrow[20\text{ min } 0^\circ\text{C}]{\text{acceptor 1 (1 eq)}}$ $\xrightarrow[5\text{ min } -78^\circ\text{C}]{p\text{-TolSCL, AgOTf}}$ $\xrightarrow[5\text{ min } -78^\circ\text{C}]{\text{acceptor 2 (0.97 eq)}}$ $\xrightarrow[20\text{ min } 0^\circ\text{C}]{}$ | | 6, 15–18 (49–58%) |
| 14 | 9 | 9 |  |
| 7 | 8 | 9 |  |
| 7 | 9 | 8 |  |
| 14 | 8 | 8 |  |
| 10 | 9 | 8 |  |

Scheme 2. Selective Deprotection and N-Acetylation



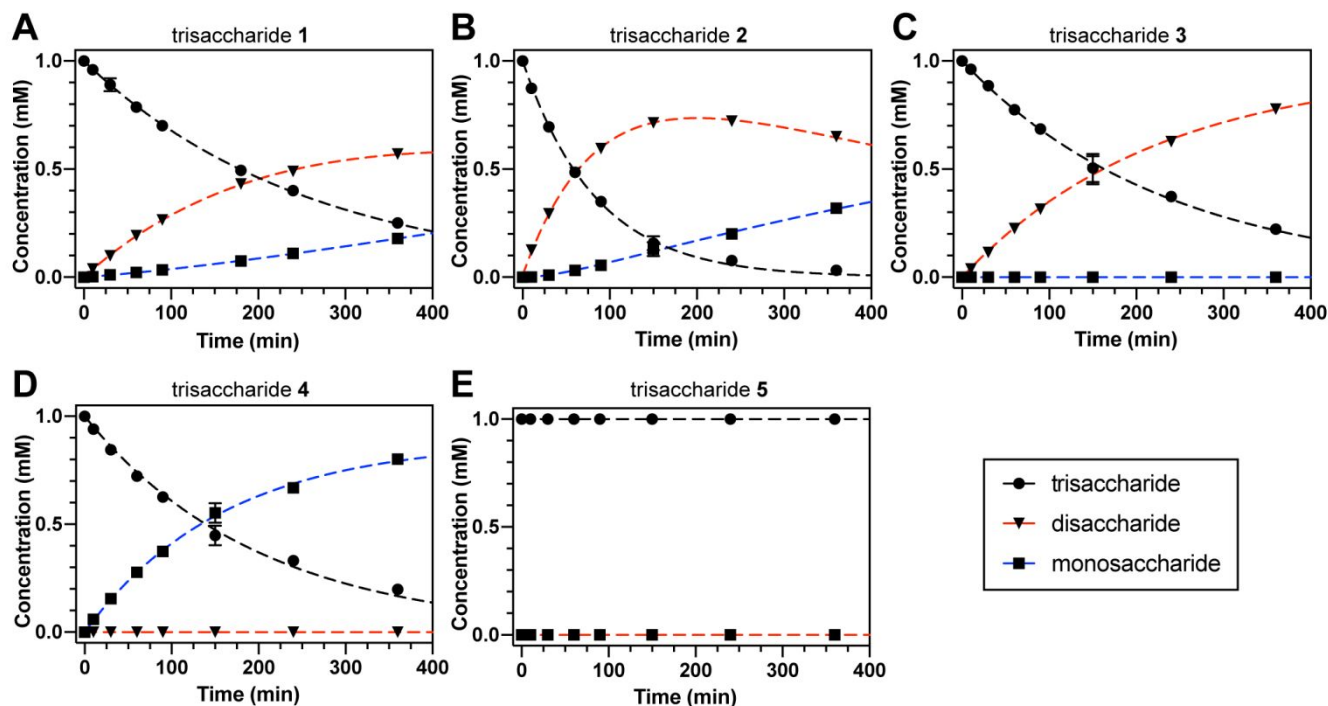


Figure 3. Time course for the hydrolysis of PNAG trisaccharide analogs **1** (A), **2** (B), **3** (C), **4** (D) and **5** (E). Lines were added to aid identification of the disappearance of the trisaccharide (black), appearance of the disaccharide (red) and appearance of the monosaccharide (blue). The concentration of remaining trisaccharide substrate and reducing-end disaccharide and monosaccharide products were determined from the relative peak areas as determined by HPLC using the *S*-tolyl aglycone absorbance at 254nm.

Table 2. Rate of trisaccharide hydrolysis catalyzed by DspB

| Trisaccharide | k_{obs} (min^{-1}) ^a |
|---------------|--|
| 1 | $3.8 \pm 0.1 \times 10^{-3}$ |
| 2 | $11.2 \pm 0.2 \times 10^{-3}$ |
| 3 | $4.0 \pm 0.2 \times 10^{-3}$ |
| 4 | $4.6 \pm 0.2 \times 10^{-3}$ |
| 5 | -- ^b |

^a Values are shown \pm the 95% confidence interval. ^b No hydrolysis products were observed over 6 h.

Product distributions from enzymatic hydrolysis by DspB. Trisaccharides **1–5** were each independently evaluated as substrates for hydrolysis by recombinant *A. actinomycetemcomitans* DspB. Substrate hydrolysis as a function of time was monitored through separation of the substrate and reducing-end products by reversed phase HPLC and monitoring the absorbance at 254 nm stemming from the *S*-tolyl aglycone. Thus, the concentration of substrate and reducing-end hydrolysis products were quantified based on their relative peak areas in HPLC chromatograms (Figure 3, Figure S1). For each reaction the product distribution was also analyzed directly by MALDI-TOF mass spectrometry to confirm product identities and identify any non-reducing end hydrolysis products lacking the *S*-tolyl aglycone (Figure S2). No evidence for aglycone cleavage from any substrate was observed by either MS or HPLC analysis. This is not surprising as thioglycosides are known to be resistant to glycosidase cleavage and 4-

nitrophenyl-GlcNAc, which contains a better leaving group as the aglycone, is a poor substrate for DspB.²³

Analysis of time points within the first 60 min for the hydrolysis of fully acetylated trisaccharide **1** by DspB showed a decrease in trisaccharide and the predominant formation of a disaccharide product (Figure 3A). This is followed by the appearance of monosaccharide and a decrease in the rate of disaccharide formation over the course of the reaction. The product distribution is consistent with primarily *exo* cleavage in which the non-reducing GlcNAc residues are cleaved in succession (Figure S3A). This is also consistent with product distributions that have been previously reported for the hydrolysis of fully acetylated PNAG oligosaccharide substrates by DspB.^{25,26} Analyzing the product distribution by MALDI-TOF MS showed only the reducing-end disaccharide product. We observed no evidence for endoglycosidic cleavage of trisaccharide **1**, which would lead directly to the formation of a nonreducing-end disaccharide product.

Next, we sought to analyze how deacetylation of the PNAG trisaccharide substrate might impact the observed product distributions. The hydrolysis of trisaccharide **2** resulted in the same product distribution observed for the hydrolysis of **1** (Figure 3B). This is again consistent with two successive cleavage of the non-reducing GlcNAc residue resulting in a GlcN-*S*-Tol monosaccharide product. With trisaccharide **3**, however, only disaccharide product formation was observed with no further hydrolysis to the monosaccharide (Figure 3C). This is in agreement with the proposed substrate assisted hydrolysis mechanism for DspB, where an *N*-Ac is required at the site of hydrolysis.^{20,23} Similarly, incubations with trisaccharide **5** containing two

nonreducing GlcN produced no hydrolysis products over the entire 6-hour time period evaluated (Figure 3E). This provides further support for a substrate assisted exoglycosidic cleavage mechanism, which requires GlcNAc at the site of cleavage common among other GH20 enzymes.⁴⁶ Given the strict requirement for an *N*-Ac at the site of cleavage, we did not anticipate much if any hydrolysis of trisaccharide **4** containing a non-reducing GlcN. However, the hydrolysis reactions resulted in a single product corresponding to a reducing-end monosaccharide (Figure 3D). The structure of this product was confirmed by co-injection with authentic monosaccharide standard (data not shown). The MALDI-TOF MS results also showed direct formation of a non-reducing end β -D-GlcN-(1 \rightarrow 6)- β -D-GlcNAc disaccharide (Figure S2).

These results afford a reasonable hypothesis for how DspB efficiently catalyzes the hydrolysis of native dPNAG biofilm polysaccharides. The enzyme functions predominantly as an exoglycosidase cleaving the non-reducing terminal GlcNAc from dPNAG polysaccharides. When a non-reducing GlcN residue is encountered, DspB is able to bypass and facilitate endo-glycosidic cleavage at the next available GlcNAc (Figure S3A). It is not clear if this activity is limited to the cleavage of a single non-reducing terminal β -D-GlcN-(1 \rightarrow 6)- β -D-GlcNAc disaccharide, or if DspB is capable of accommodating longer oligosaccharides down from the site of cleavage. Further studies with longer dPNAG analogs are still required to differentiate these possibilities.

Differential rate of trisaccharide hydrolysis by DspB. We attempted to measure steady state kinetic parameters to gain more mechanistic insight into the DspB catalyzed hydrolysis of trisaccharide analogs **1** and **2**. For all concentrations tested (0.1–5 mM), we observed a linear increase in the initial velocity with concentration suggesting that even 5 mM trisaccharide is well below K_M (Figure S4A). This was unexpected as related GH20 enzymes have K_M values in the 0.1–1 mM range.^{47,48} Instead, the DspB catalytic efficiencies for **1–5** were determined from the observed rate constants (k_{obs}) for disappearance of trisaccharide by fitting reaction progress curves to a single exponential (eq 1). Here $[S]$ is the trisaccharide substrate concentration, $[S_0]$ is the initial trisaccharide concentration, and t is time. Under conditions where $[S_0] \leq K_M$ a single exponential fit to the reaction progress curve (k_{obs}) is proportional to the enzyme specificity constant V/K , but does not allow for unambiguous determination of K_M and V_{max} .⁴⁹ Thus, k_{obs} represents a pseudo-first-order rate constant for hydrolysis of the trisaccharide that can be used to directly compare DspB catalytic efficiency with different substrates.

$$[S] = [S_0] \times e^{(-k_{obs}t)} \quad (1)$$

Surprisingly, the hydrolysis of trisaccharide **1**, **3** and **4** showed little variation in the observed rates (Table 2, Figure S4B) despite the differences in product distribution that were obtained in HPLC and MS measurements. These rates are of similar magnitude to those reported previously for DspB hydrolysis of fully acetylated PNAG oligomers ranging in size from disaccharides to pentasaccharides.²⁶ Thus, it appears as though the rate of hydrolysis is not significantly impacted by de-acetylation of the substrate in either the +1 or -2 binding sites (Figure S3B). Reaction of

DspB with trisaccharide **2** resulted in an observed rate of hydrolysis ~2.5-fold greater than observed for any other trisaccharide analog. This demonstrates a preferential turnover of substrates with GlcN located in the +2 binding site of DspB. To verify this observed substrate preference, internal competition experiments in which both trisaccharide **1** and **2** were co-incubated with DspB were performed (Figure S5). Here, the same substrate preference was observed with the rate of trisaccharide **2** consumption being ~3-fold faster than trisaccharide **1** co-incubated in the same hydrolysis reaction. Taking this data together it is clear that DspB shows a preference for GlcN in the +2-position relative to the site of cleavage, but that this is not a strict requirement for substrate hydrolysis. It is possible that the preference for GlcN in the +2 binding site allows for more efficient recognition of dPNAG polysaccharides.

DspB and PgaB utilize different mechanism for dPNAG hydrolysis. Hydrolysis of dPNAG by PgaB proceeds exclusively via an endo-glycosidic cleavage mechanism and requires GlcN, and GlcNAc in the -3 and -1 binding sites, respectively.²² In this case de-*N*-acetylation is essential for PgaB hydrolytic activity. By comparison, the results from hydrolysis of **1–5** by DspB support a mechanism where DspB is capable of hydrolyzing dPNAG through either exo- or endo-glycosyl hydrolysis mechanisms depending on the substrate acetylation pattern.

The different mechanisms employed by PgaB and DspB may relate to their different biological roles in the biofilm lifecycle. PgaB is localized in the periplasm as part of the biosynthetic machinery required for dPNAG assembly and export.¹⁰ It contains both the C-terminal GH153 domain and a N-terminal carbohydrate esterase domain, which catalyzes the de-*N*-acetylation of PNAG.^{12,22,50} It is still not clear what biological role this hydrolytic activity plays, if any, during dPNAG biosynthesis. DspB, on the other hand, is a secreted protein that functions in *A. actinomycetemcomitans* biofilm dispersal. A transposon insertion mutant of *A. actinomycetemcomitans* that disrupts DspB expression displays a phenotype deficient in biofilm cell detachment.¹⁷ The ability of DspB to effectively catalyze both exo- and endo-glycosidic cleavage reactions would allow for more efficient dPNAG hydrolysis during biofilm dispersal.

DspB has a charged substrate binding surface. Additional insight into the origin of this observed specificity was gained by comparing the binding site of DspB to other GH20 family glycosyl hydrolase enzymes. An analysis of the DspB structure using the DALI server identified the tandem GH20 domains of StrH as the closest structural homologues.⁵¹ The GH20 domains of StrH catalyze the hydrolysis of terminal GlcNAc residues of N-glycan and functions as a major virulence factor in Pneumococcal species.⁴⁷ The overlay in Figure 4A shows the apo structure of DspB compared to that of StrH bound to a N-glycan tetrasaccharide substrate.^{20,47} StrH and DspB share 23% overall sequence identity and all of the active site residues involved in recognition of the non-reducing GlcNAc in the -1 binding site are conserved with the exception of Asp56 and Trp216, which correspond to Asn670 and Phe849 in StrH. Therefore, it is likely that the GlcNAc residue in the -1 binding site is bound in a similar conformation in both

proteins. Compared to StrH, the predicted binding surface of DspB is more open and displays a net negative charge (Figure 4B–C). This anionic surface of DspB may function in recognition of positively charged GlcN

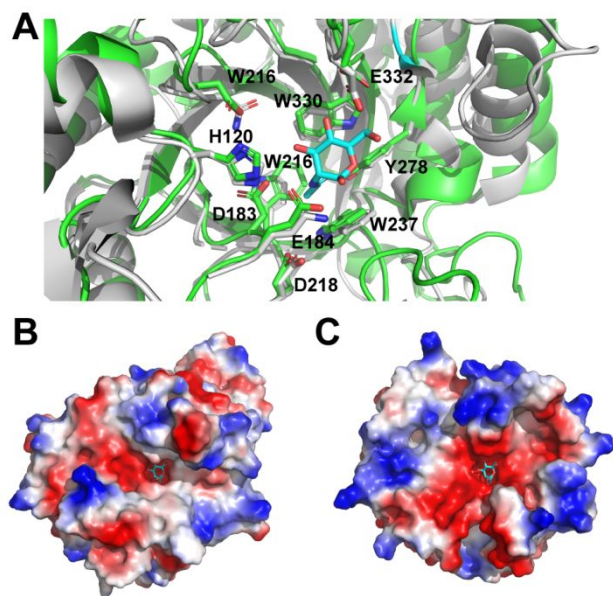


Figure 4. Structural comparison of DspB with other GH20 enzymes. (A) Overlay of DspB apo structure (PDB 1YHT, green) with StrH (PDB 2YL9, grey). The GlcNAc in the -1 site of StrH is shown (cyan). Select active site residues of DspB are highlighted. Electrostatic surface maps for StrH (B) and DspB (C) showing positive surface charge in blue and negative surface charge in red. The GlcNAc at the -1 binding site of StrH is shown and is modeled in the active site of DspB (cyan).

present in native dPNAG and explain the preferential recognition of substrates with GlcN in the +2 binding site. A similar charged surface is also present in the binding site of PgaB indicating that this may be a general feature of dPNAG specific GH enzymes.²² It is not clear from this study if the preference for recognition of GlcN over GlcNAc limited to the +2 subsite or if there are additional binding sites for recognition of GlcN. Thus, further work is required to specifically characterize the conformation of bound dPNAG in the active site of DspB and identify specific interactions of the +2 and -2 binding sites. Understanding how glycosidase enzymes like DspB interact with their exopolysaccharide substrates is not only critical for their development as biocatalysts but will provide critical insight into the process of EPS breakdown during the natural process of biofilm dispersal and may lead to the identification of novel dPNAG specific β -hexosaminidase enzymes.

CONCLUSIONS

A robust one-pot glycosylation approach has been developed to assemble dPNAG trisaccharides with specific acetylation patterns from easily accessible building blocks. Trisaccharides with defined acetylation patterns can be obtained in good yield by simply varying the order of reagent addition during the one-pot glycosylation. Inclusion of a 6-*O*-Fmoc protecting group allows the trisaccharide

product to be converted into both glycosyl donors or acceptors for further glycosylation reactions. All trisaccharide products synthesized served as effective probes for DspB hydrolytic activity. From the results of these studies it is clear that DspB activity and product distributions are dependent on substrate acetylation patterns. Specifically, de-*N*-acetylation in the +2 position of dPNAG trisaccharide resulted in an increase in substrate hydrolysis by DspB. The enhanced rate of hydrolysis was not observed for deacetylation at other positions, indicating that dPNAG with specific acetylation patterns are preferentially recognized. The hydrolysis product distributions observed are consistent with primarily exo- β -*D*-*N*-acetylglucosaminidase activity using substrate assisted hydrolysis for substrates containing non-reducing GlcNAc. However, DspB can also catalyze endo-glycosidic cleavage at nearly identical rate for substrates containing GlcN at the -2 binding site. These results imply that DspB hydrolysis of dPNAG polysaccharides can proceed via either exo- or endoglycosidase mechanisms depending on the specific substrate acetylation pattern, but further studies are required to characterize the substrate binding interactions in greater detail. As DspB is one of only a few enzymes known to degrade dPNAG, understanding its activity and specificity is crucial for our understanding of biofilm dispersal.

MATERIALS AND METHODS

DspB-catalyzed hydrolysis of PNAG trisaccharide analogs. Hydrolysis reactions containing final concentrations of 15 μ M His₆-DspB and 1 mM trisaccharide (1–5) in a buffer of 50 mM potassium phosphate, pH 6.0, with 100 mM NaCl in a 50 μ L final volume. The reaction was initiated through the addition of His₆-DspB, and incubated at 22°C. Aliquots of 5 μ L were removed after 0 min, 10 min, 30 min, 60 min, 90 min, 150 min, 240 min and 360 min incubation and quenched through addition of 5 μ L of 100 mM trifluoroacetic acid (TFA). Quenched fractions were centrifuged at 17,000 \times g for 2 min to pellet any insoluble material and 5 μ L of supernatant was diluted to a final volume of 50 μ L with MQ water for HPLC analysis. Samples were separated on a Kinetex C18 column (150 \times 4.6 mm, 5 μ m) at 1 mL/min flow rate using a linear gradient elution from 0.1% formic acid (buffer A) to 50% acetonitrile (buffer B) over 12 min. The column was washed with buffer B for 4 min and then re-equilibrated with buffer A for 4 min before subsequent injections. Analytes were observed using the absorbance at 254 nm resulting from the *S*-tolyl aglycone. Concentrations of residual substrate and reducing-end hydrolysis products were determined from their relative peak areas, which were plotted as a function of time to obtain the reaction time course. Analyte concentrations from two independent experiments were averaged to obtain reaction time course data.

Initial velocity measurements were carried out using the same activity assay but with varying trisaccharide concentrations between 0.1–5 mM. Reaction aliquots were removed and quenched at 5, 10, 20 and 30 min time points and initial velocities were determined from the linear portion of the reaction progress curve.

The direct competitive hydrolysis of **1** and **2** was measured using a reaction mixture of 15 μ M His₆-DspB containing both 1 mM trisaccharide **1** and 1 mM trisaccharide **2** in a final volume of 50 μ L of 50 mM potassium phosphate, pH 6.0, 100 mM NaCl. The reactions were analyzed as described above.

Product analysis by MALDI-TOF mass spectrometry.

DspB reaction mixtures were prepared as described above. Quenched reaction aliquots for MALDI-TOF MS analysis were directly spotted as a 1:1 mixture with DHB matrix. Spectra were recorded in positive reflectron mode using a Bruker Autoflex Speed mass spectrometer. Laser power was adjusted to be above threshold to obtain good resolution and signal/background ratios. Spectra were gathered for 3000 shots total to ensure the normalization of peak ratios during data collection.

ASSOCIATED CONTENT

Supporting Information

The Supporting Information is available free of charge on the ACS Publications website.

Methods for synthesis of trisaccharides **1–5**, experimental protocols for protein production, supplemental figures, and spectral data for all new compounds (PDF)

AUTHOR INFORMATION

Corresponding Author

* mpoulin@umd.edu

Author Contributions

The manuscript was written through contributions of all authors. All authors have given approval to the final version of the manuscript.

Notes

The authors declare no competing financial interests.

ACKNOWLEDGMENT

We are grateful to the University of Maryland College Park for startup funds. We thank F. Chen and Y. Li for help with analytical NMR and mass spectrometry services. We thank D. Fushman, and J. Davis for helpful discussion.

REFERENCES

- (1) Joo, H.-S., and Otto, M. (2012) Molecular basis of in vivo biofilm formation by bacterial pathogens. *Chem. Biol.* **19**, 1503–1513.
- (2) Mack, D., Fischer, W., Krokotsch, A., Leopold, K., Hartmann, R., Egge, H., and Laufs, R. (1995) The intercellular adhesin involved in biofilm accumulation of *Staphylococcus epidermidis* is a linear β -1,6-linked glucosaminoglycan: purification and structural analysis. *J. Bacteriol.* **178**, 175–183.
- (3) Cramton, S. E., Gerke, C., Schnell, N. F., Nichols, W. W., and Götz, F. (1999) The intercellular adhesion (*ica*) locus is present in *Staphylococcus aureus* and is required for biofilm formation. *Infect. Immun.* **67**, 5427–5433.
- (4) Wang, X., Preston, J. F., and Romeo, T. (2004) The pgaABCD locus of *Escherichia coli* promotes the synthesis of a polysaccharide adhesin required for biofilm formation. *J. Bacteriol.* **186**, 2724–2734.
- (5) Choi, A. H. K., Slamti, L., Avci, F. Y., Pier, G. B., and Mair-Litran, T. (2009) The pgaABCD locus of *Acinetobacter baumannii*

encodes the production of poly- β -1-6-*N*-acetylglucosamine, which is critical for biofilm formation. *J. Bacteriol.* **191**, 5953–5963.

(6) Izano, E. A., Sadovskaya, I., Vinogradov, E., Mulks, M. H., Velliagounder, K., Raganath, C., Kher, W. B., Ramasubbu, N., Jabbouri, S., Perry, M. B., and Kaplan, J. B. (2007) Poly-*N*-acetylglucosamine mediates biofilm formation and antibiotic resistance in *Actinobacillus pleuropneumoniae*. *Microb. Pathog.* **43**, 1–9.

(7) Chen, K.-M., Chiang, M.-K., Wang, M., Ho, H.-C., Lu, M.-C., and Lai, Y.-C. (2014) The role of pgaC in *Klebsiella pneumoniae* virulence and biofilm formation. *Microb. Pathog.* **77**, 89–99.

(8) Jarrett, C. O., Deak, E., Isherwood, K. E., Oyston, P. C., Fischer, E. R., Whitney, A. R., Kobayashi, S. D., DeLeo, F. R., and Hinnebusch, B. J. (2004) Transmission of *Yersinia pestis* from an infectious biofilm in the flea vector. *J. Infect. Dis.* **190**, 783–792.

(9) Vuong, C., Kocianova, S., Voyich, J. M., Yao, Y., Fischer, E. R., DeLeo, F. R., and Otto, M. (2004) A crucial role for exopolysaccharide modification in bacterial biofilm formation, immune evasion, and virulence. *J. Biol. Chem.* **279**, 54881–54886.

(10) Itoh, Y., Rice, J. D., Goller, C., Pannuri, A., Taylor, J., Meisner, J., Beveridge, T. J., Preston, J. F., and Romeo, T. (2008) Roles of pgaABCD genes in synthesis, modification, and export of the *Escherichia coli* biofilm adhesin poly- β -1,6-*N*-acetyl-D-glucosamine. *J. Bacteriol.* **190**, 3670–3680.

(11) Little, D. J., Milek, S., Bamford, N. C., Ganguly, T., DiFrancesco, B. R., Nitz, M., and Howell, P. L. (2015) The protein BpsB is a poly- β -1,6-*N*-acetyl-D-glucosamine deacetylase required for biofilm formation in *Bordetella bronchiseptica*. *J. Biol. Chem.* **290**, 22827–22840.

(12) Little, D. J., Bamford, N. C., Pokrovskaya, V., Robinson, H., Nitz, M., and Howell, P. L. (2014) Structural basis for the de-*N*-acetylation of poly- β -1,6-*N*-acetyl-D-glucosamine in gram-positive bacteria. *J. Biol. Chem.* **289**, 35907–35917.

(13) Baker, P., Hill, P. J., Snarr, B. D., Alnabseya, N., Pestrak, M. J., Lee, M. J., Jennings, L. K., Tam, J., Melnyk, R. A., Parsek, M. R., Sheppard, D. C., Wozniak, D. J., and Howell, P. L. (2016) Exopolysaccharide biosynthetic glycoside hydrolases can be utilized to disrupt and prevent *Pseudomonas aeruginosa* biofilms. *Sci. Adv.* **2**, e1501632.

(14) Kaplan, J. B., Mlynek, K. D., Hettiarachchi, H., Alamneh, Y. A., Biggemann, L., Zurawski, D. V., Black, C. C., Bane, C. E., Kim, R. K., and Granick, M. S. (2018) Extracellular polymeric substance (EPS)-degrading enzymes reduce staphylococcal surface attachment and biocide resistance on pig skin *in vivo*. *PLoS ONE* **13**, e0205526.

(15) Fey, P. D. (2010) Modality of bacterial growth presents unique targets: how do we treat biofilm-mediated infections? *Curr. Opin. Microbiol.* **13**, 610–615.

(16) Asker, D., Awad, T. S., Baker, P., Howell, P. L., and Hatton, B. D. (2018) Non-eluting, surface-bound enzymes disrupt surface attachment of bacteria by continuous biofilm polysaccharide degradation. *Biomaterials* **167**, 168–176.

(17) Kaplan, J. B., Raganath, C., Ramasubbu, N., and Fine, D. H. (2003) Detachment of *Actinobacillus actinomycetemcomitans* biofilm cells by an endogenous β -hexosaminidase activity. *J. Bacteriol.* **185**, 4693–4698.

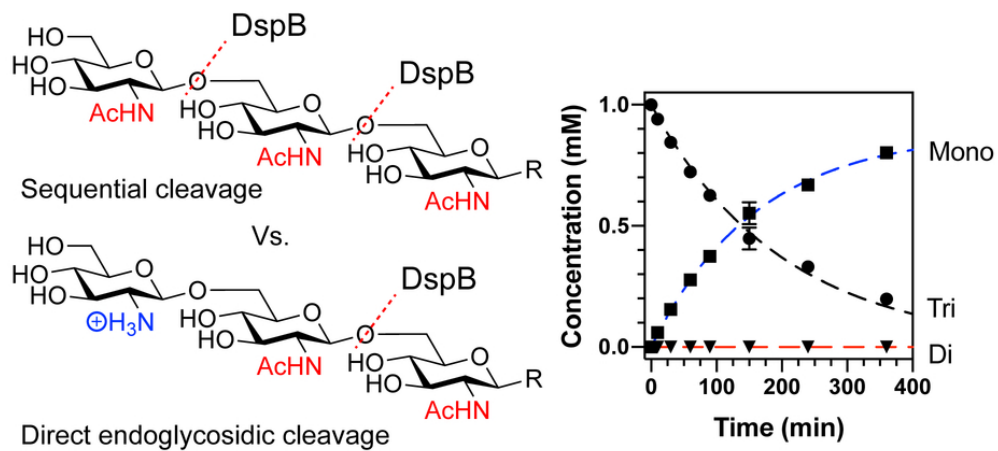
(18) Kaplan, J. B., Raganath, C., Velliagounder, K., Fine, D. H., and Ramasubbu, N. (2004) Enzymatic detachment of *Staphylococcus epidermidis* biofilms. *Antimicrob. Agents Chemother.* **48**, 2633–2636.

(19) Itoh, Y., Wang, X., Hinnebusch, B. J., Preston, J. F., and Romeo, T. (2005) Depolymerization of β -1,6-*N*-acetyl-D-glucosamine disrupts the integrity of diverse bacterial biofilms. *J. Bacteriol.* **187**, 382–387.

(20) Ramasubbu, N., Thomas, L. M., Raganath, C., and Kaplan, J. B. (2005) Structural analysis of Dispersin B, a biofilm-releasing glycoside hydrolase from the periodontopathogen *Actinobacillus actinomycetemcomitans*. *J. Mol. Biol.* **349**, 475–486.

(21) Lombard, V., Golaconda Ramulu, H., Drula, E., Coutinho, P.

- M., and Henrissat, B. (2013) The carbohydrate-active enzymes database (CAZy) in 2013. *Nucl. Acids Res.* *42*, D490–D495.
- (22) Little, D. J., Pfoh, R., Le Mauff, F., Bamford, N. C., Notte, C., Baker, P., Guragain, M., Robinson, H., Pier, G. B., Nitz, M., Deora, R., Sheppard, D. C., and Howell, P. L. (2018) PgaB orthologues contain a glycoside hydrolase domain that cleaves deacetylated poly- β (1,6)-*N*-acetylglucosamine and can disrupt bacterial biofilms. *PLoS Pathog.* *14*, e1006998.
- (23) Manuel, S. G. A., Rangunath, C., Sait, H. B. R., Izano, E. A., Kaplan, J. B., and Ramasubbu, N. (2007) Role of active-site residues of Dispersin B, a biofilm-releasing β -hexosaminidase from a periodontal pathogen, in substrate hydrolysis. *FEBS J.* *274*, 5987–5999.
- (24) Greig, I. R., Zahariev, F., and Withers, S. G. (2008) Elucidating the nature of the *Streptomyces plicatus* β -hexosaminidase-bound intermediate using *ab initio* molecular dynamics simulations. *J. Am. Chem. Soc.* *130*, 17620–17628.
- (25) Fekete, A., Borbás, A., Gyémánt, G., Kandra, L., Fazekas, E., Ramasubbu, N., and Antus, S. (2011) Synthesis of β -(1,6)-linked *N*-acetyl-D-glucosamine oligosaccharide substrates and their hydrolysis by Dispersin B. *Carbohydr. Res.* *346*, 1445–1453.
- (26) Fazekas, E., Kandra, L., and Gyémánt, G. (2012) Model for β -1,6-*N*-acetylglucosamine oligomer hydrolysis catalysed by Dispersin B, a biofilm degrading enzyme. *Carbohydr. Res.* *363*, 7–13.
- (27) Whitfield, G. B., Marmont, L. S., and Howell, P. L. (2015) Enzymatic modifications of exopolysaccharides enhance bacterial persistence. *Front. Microbiol.* *6*, 7350–21.
- (28) Yang, F., and Du, Y. (2003) A practical synthesis of a (1 \rightarrow 6)-linked β -D-glucosamine nonasaccharide. *Carbohydr. Res.* *338*, 495–502.
- (29) Chen, Q., Yang, F., and Du, Y. (2005) Synthesis of a C3-symmetric (1 \rightarrow 6)-*N*-acetyl- β -D-glucosamine octadecasaccharide using click chemistry. *Carbohydr. Res.* *340*, 2476–2482.
- (30) Gening, M. L., Tsvetkov, Y. E., Pier, G. B., and Nifantiev, N. E. (2007) Synthesis of β -(1 \rightarrow 6)-linked glucosamine oligosaccharides corresponding to fragments of the bacterial surface polysaccharide poly-*N*-acetylglucosamine. *Carbohydr. Res.* *342*, 567–575.
- (31) Gening, M. L., Tsvetkov, Y. E., Titov, D. V., Gerbst, A. G., Yudina, O. N., Grachev, A. A., Shashkov, A. S., Vidal, S., Imbert, A., Saha, T., Kand, D., Talukdar, P., Pier, G. B., and Nifantiev, N. E. (2013) Linear and cyclic oligo- β -(1,6)-D-glucosamines: Synthesis, conformations, and applications for design of a vaccine and oligodentate glycoconjugates. *Pure Appl. Chem.* *85*, 175–14.
- (32) Weaver, L. G., Singh, Y., Blanchfield, J. T., and Burn, P. L. (2013) A simple iterative method for the synthesis of β -(1,6)-glucosamine oligosaccharides. *Carbohydr. Res.* *371*, 68–76.
- (33) Leung, C., Chibba, A., Gómez-Biagi, R. F., and Nitz, M. (2009) Efficient synthesis and protein conjugation of β -(1 \rightarrow 6)-D-*N*-acetylglucosamine oligosaccharides from the polysaccharide intercellular adhesin. *Carbohydr. Res.* *344*, 570–575.
- (34) Fridman, M., Solomon, D., Yoge, S., and Baasov, T. (2002) One-pot synthesis of glucosamine oligosaccharides. *Org. Lett.* *4*, 281–283.
- (35) Melean, L. G., Love, K. R., and Seeberger, P. H. (2002) Toward the automated solid-phase synthesis of oligoglucosamines: systematic evaluation of glycosyl phosphate and glycosyl trichloroacetimidate building blocks. *Carbohydr. Res.* *337*, 1893–1916.
- (36) Ko, K.-S., Park, G., Yu, Y., and Pohl, N. L. (2008) Protecting-group-based colorimetric monitoring of fluoruous-phase and solid-phase synthesis of oligoglucosamines. *Org. Lett.* *10*, 5381–5384.
- (37) Nokami, T., Hayashi, R., Saigusa, Y., Shimizu, A., Liu, C.-Y., Mong, K.-K. T., and Yoshida, J.-I. (2013) Automated solution-phase synthesis of oligosaccharides via iterative electrochemical assembly of thioglycosides. *Org. Lett.* *15*, 4520–4523.
- (38) Kanno, K. I., and Hatanaka, K. (2005) Synthesis of 1,6-Anhydro-4-*O*-benzyl-2-deoxy-3-*O*-p-methoxybenzoyl-2-phalimido- β -D-glucopyranose and its oligomers. *Polym. J.* *30*, 678–680.
- (39) Yudina, O. N., Gening, M. L., Tsvetkov, Y. E., Grachev, A. A., Pier, G. B., and Nifantiev, N. E. (2011) Synthesis of five nona- β -(1,6)-D-glucosamines with various patterns of *N*-acetylation corresponding to the fragments of exopolysaccharide of *Staphylococcus aureus*. *Carbohydr. Res.* *346*, 905–913.
- (40) Huang, X., Huang, L., Wang, H., and Ye, X.-S. (2004) Iterative one-pot synthesis of oligosaccharides. *Angew. Chem. Int. Ed.* *43*, 5221–5224.
- (41) Dulaney, S. B., Xu, Y., Wang, P., Tiruchinapally, G., Wang, Z., Kathawa, J., El-Dakdouki, M. H., Yang, B., Liu, J., and Huang, X. (2015) Divergent synthesis of heparan sulfate oligosaccharides. *J. Org. Chem.* *80*, 12265–12279.
- (42) Wu, Y., Xiong, D.-C., Chen, S.-C., Wang, Y.-S., and Ye, X.-S. (2017) Total synthesis of mycobacterial arabinogalactan containing 92 monosaccharide units. *Nat. Commun.* *8*, 1–7.
- (43) Grann Hansen, S., and Skrydstrup, T. (2007) Studies directed to the synthesis of oligochitosans – preparation of building blocks and their evaluation in glycosylation studies. *Eur. J. Org. Chem.* *2007*, 3392–3401.
- (44) Ren, B., Cai, L., Zhang, L.-R., Yang, Z.-J., and Zhang, L.-H. (2005) Selective deacetylation using iodine-methanol reagent in fully acetylated nucleosides. *Tetrahedron Lett.* *46*, 8083–8086.
- (45) Lu, S.-R., Lai, Y.-H., Chen, J.-H., Liu, C.-Y., and Mong, K.-K. T. (2011) Dimethylformamide: An unusual glycosylation modulator. *Angew. Chem. Int. Ed.* *50*, 7315–7320.
- (46) Mark, B. L., Vocadlo, D. J., Knapp, S., Triggs-Raine, B. L., Withers, S. G., and James, M. N. G. (2001) Crystallographic evidence for substrate-assisted catalysis in a bacterial β -hexosaminidase. *J. Biol. Chem.* *276*, 10330–10337.
- (47) Jiang, Y.-L., Yu, W.-L., Zhang, J.-W., Frolet, C., Di Guilmi, A.-M., Zhou, C.-Z., Vernet, T., and Chen, Y. (2011) Structural basis for the substrate specificity of a novel β -*N*-acetylhexosaminidase StrH protein from *Streptococcus pneumoniae* R6. *J. Biol. Chem.* *286*, 43004–43012.
- (48) Ito, T., Katayama, T., Hattie, M., Sakurama, H., Wada, J., Suzuki, R., Ashida, H., Wakagi, T., Yamamoto, K., Stubbs, K. A., and Fushinobu, S. (2013) Crystal structures of a glycoside hydrolase family 20 lacto-*N*-biosidase from *Bifidobacterium bifidum*. *J. Biol. Chem.* *288*, 11795–11806.
- (49) Stroberg, W., and Schnell, S. (2016) On the estimation errors of KM and V from time-course experiments using the Michaelis–Menten equation. *Biophys. Chem.* *219*, 17–27.
- (50) Little, D. J., Poloczek, J., Whitney, J. C., Robinson, H., Nitz, M., and Howell, P. L. (2012) The structure- and metal-dependent activity of *Escherichia coli* PgaB provides insight into the partial de-*N*-acetylation of poly- β -1,6-*N*-acetyl-D-glucosamine. *J. Biol. Chem.* *287*, 31126–31137.
- (51) Holm, L., and Laakso, L. M. (2016) Dali server update. *Nucl. Acids Res.* *44*, W351–W355.



78x38mm (300 x 300 DPI)